Cancer Research

Ablation of TAK1 Upregulates Reactive Oxygen Species and Selectively Kills Tumor Cells

Emily Omori[1], Kunihiro Matsumoto[2], Songyun Zhu[1], Robert C. Smart[1], and Jun Ninomiya-Tsuji[1]

Abstract

TAK1 kinase activates multiple transcription factors and regulates the level of reactive oxygen species (ROS). We have previously reported that ablation of TAK1 in keratinocytes causes hypersensitivity to ROS-induced cell apoptosis. It is known that some tumor cells produce ROS at higher levels compared with normal cells. We used inducible epidermal-specific TAK1 knockout mice and examined whether ablation of TAK1 in preexisting skin tumors could cause an increase in ROS and result in tumor cell death. Deletion of *tak1* gene in skin tumors caused the accumulation of ROS and increased apoptosis, and skin tumors totally regressed within 5 to 10 days. Normal skin did not exhibit any significant abnormality on *tak1* gene deletion. Thus, TAK1 kinase could be a new and effective molecular target for ROS-based tumor killing. *Cancer Res; 70(21); 8417–25. ©2010 AACR.*

Introduction

TAK1 is a member of mitogen-activated protein kinase (MAPK) kinase kinase (MAPKKK) and is an indispensable signaling intermediate in several MAPK and NF-κB pathways (1–3). In mouse models, TAK1 is found to be essential for immune cell differentiation and activation by mediating activation of MAPK and NF-κB (4–7). In epithelial cells, we have shown that TAK1 is critically involved in cell survival and that ablation of TAK1 upregulates tumor necrosis factor (TNF)–induced epithelial cell death (8–10). Ablation of TAK1 signaling diminishes activation of MAPK and NF-κB pathways, and decreases antioxidant capacity (9). Reactive oxygen species (ROS) accumulation and apoptosis are observed on TNF stimulation in cultured TAK1-deficient epidermal cells (keratinocytes; ref. 9).

Cells constantly generate ROS as byproducts of energy metabolism through the electron transport chain reactions in mitochondria. Environmental factors such as commensal bacteria and stressors can additionally upregulate ROS generation in the cells. Thus, cellular antioxidant systems including TAK1 pathway are thought to be required for protecting cells from ROS-induced cell damage. Indeed, ablation of TAK1 spontaneously causes severe tissue damage in the intestinal epithelium (8). Neonatal mice having epidermal-specific constitutive deletion of TAK1 also exhibit severe skin damage (10). Thus, the TAK1 pathway is important for cell survival for some epithelial tissues. In contrast, adult mice having inducible epidermal-specific deletion of TAK1 exhibit mild tissue damage and moderately elevated apoptosis on *tak1* gene deletion (9). Cultured TAK1-deficient fibroblasts and keratinocytes grow normally and do not exhibit significantly increased ROS (9). Thus, under the standard tissue culture conditions as well as in the adult skin, the TAK1 pathway is not always required for cell survival.

It is well known that tumor cells produce ROS at higher levels compared with normal cells because tumors have increased energy metabolism and other abnormalities such as oncogenic stress and mitochondrial dysfunction, which are associated with increased ROS production (11). Because of the increased intracellular levels of ROS, some tumor cells are hypersensitive to oxidative stress (12–14). However, tumor cells often upregulate cellular levels of antioxidant to counteract increased ROS levels (15). By decreasing the cellular antioxidant capacity in tumor cells, the increased levels of endogenous ROS production could result in tumor cell death. We hypothesized that ablation of TAK1 would decrease cellular antioxidant capacity in tumors, cause increased levels of ROS, and kill tumor cells. In this study, we tested the hypothesis that TAK1 ablation selectively kills tumor cells via ROS in a skin tumor model.

Materials and Methods

Mice

TAK1-floxed ($TAK1^{flox/flox}$) mice were from Dr. Akira (Osaka University; ref. 6). *K14-CreERT* mice were obtained from The Jackson Laboratory (16). Mice harboring an epidermal-specific inducible TAK1 deletion (*K14-CreERT* $TAK1^{flox/flox}$) were generated, and *tak1* gene deletion was examined by PCR as described previously (9). Littermate controls were used in all experiments. All animal experiments were done with the approval of the North Carolina State University Institutional Animal Care and Use Committee.

Authors' Affiliations: [1]Department of Environmental and Molecular Toxicology, North Carolina State University, Raleigh, North Carolina and [2]Department of Molecular Biology, Graduate School of Science, Nagoya University, Nagoya, Japan

Corresponding Author: Jun Ninomiya-Tsuji, Department of Environmental and Molecular Toxicology, North Carolina State University, Campus Box 7633, Raleigh, NC 27695-7633. Phone: 919-513-1586; Fax: 919-515-7169; E-mail: Jun_Tsuji@ncsu.edu.

doi: 10.1158/0008-5472.CAN-10-1227

Cell culture and reagents

T24 cells were purchased from the American Type Culture Collection (ATCC; HBT-4) and cultured in DMEM supplemented with 10% bovine growth serum (Hyclone) and penicillin-streptomycin at 37°C in 5% CO_2. Less than six times passaged T24 cells after purchase were used. ATCC characterized the cells by using isoenzymology and/or the cytochrome *c* subunit I PCR assay and short tandem repeat analyses. Reagents used were tamoxifen (MP) 7,12-dimethylbenz(a)anthracene (DMBA; Acros), 12-*O*-tetradecanoylphorbol-13-acetate (TPA; LC Laboratories), 5Z-7-oxozeaenol (17), Bouin fixation fluid (EMD), anti–poly(ADP-ribose) polymerase (PARP; Cell Signaling), and anti-bromodeoxyuridine (BrdUrd; Abcam).

Tumor experiments

Control (*TAK1*$^{flox/flox}$) and inducible epidermal-specific TAK1 deletion (*K14-CreERT TAK1*$^{flox/flox}$) mouse littermates (6–9 weeks old) were treated with a single application of 200 nmol DMBA followed 1 week later with three treatments each week of 5 nmol TPA for 19 to 27 weeks (18). All agents were applied in 200 μL acetone. For a tumor regression assay, TPA treatment was terminated and 0.5 to 1 mg/mouse tamoxifen was i.p. injected for 5 consecutive days. The fifth day of tamoxifen injection is designated as day 0. To test the effect of TAK1 inhibition in skin papilloma development, CD1 mice were given a single application of 200 nmol DMBA followed 1 week later with twice-weekly treatment of acetone + 5 nmol TPA or 100 nmol 5Z-7-oxozeaenol + 5 nmol TPA for 25 weeks. TPA was administered 30 minutes after acetone or 5Z-7-oxozeaenol treatment.

Immunohistochemistry

Terminal deoxynucleotidyl transferase–mediated dUTP nick end labeling (TUNEL) assay was performed on Bouin-fixed

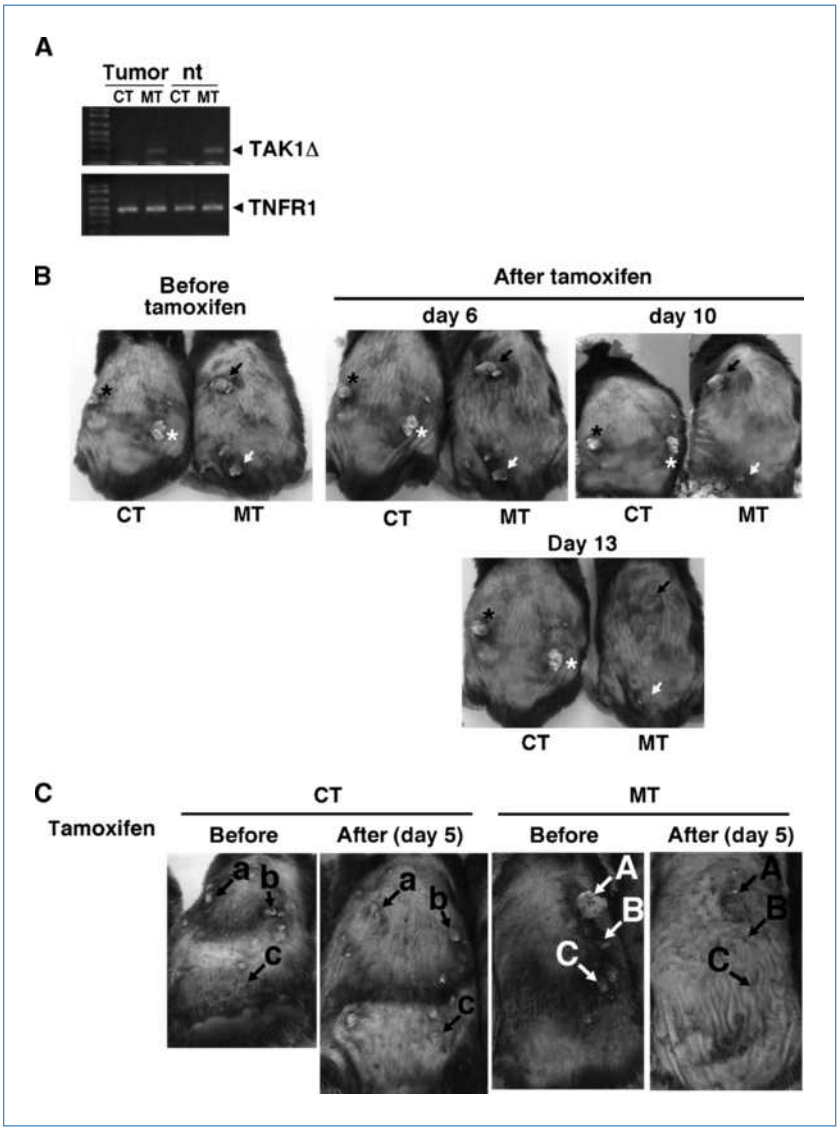

Figure 1. Skin tumors regress by *tak1* gene deletion. A, *tak1* gene deletion was examined in tumors or normal region of the skin (nt) at 7 d after tamoxifen treatment (0.5 mg/mouse/day for 5 consecutive days). Primers used were capable of amplifying only the shorter *tak1* gene after Cre-mediated recombination. TNFR1 gene was used as a loading control (9). CT, *TAK1*$^{flox/flox}$; MT, *K14-CreERT TAK1* $^{flox/flox}$. B, tumors in the same mice before and after tamoxifen treatment. Skin papillomas were induced by DMBA and TPA method. Four *TAK1*$^{flox/flox}$ (CT) and five *K14-CreERT TAK1* $^{flox/flox}$ (MT) mice were treated with tamoxifen (0.5 mg/mouse/day) for 5 consecutive days. The tumors were monitored right before the initiation of the tamoxifen injection and 6, 10, and 13 d after the tamoxifen treatment. All tumors in MT mice completely regressed by 13 to 14 d after the tamoxifen injection. Representative pictures are shown. The asterisk or arrow indicates the same tumor. Sizes of tumors shown before tamoxifen were 2 to 8 mm in diameter. C, similar experiments as A were performed using a slightly different treatment regimen. Six *TAK1*$^{flox/flox}$ (CT) and six *K14-CreERT TAK1* $^{flox/flox}$ (MT) mice having skin papillomas were treated with tamoxifen (1 mg/mouse/day) for 5 consecutive days. The tumors were monitored right before the initiation of the tamoxifen injection (before) and 4 d after the tamoxifen treatment (after). All tumors in MT mice regressed by 4 d after the tamoxifen injection. Representative pictures of a CT and MT mouse are shown. Each labeled arrow indicates the same tumor. Sizes of tumors shown before tamoxifen were 1 to 8 mm in diameter.

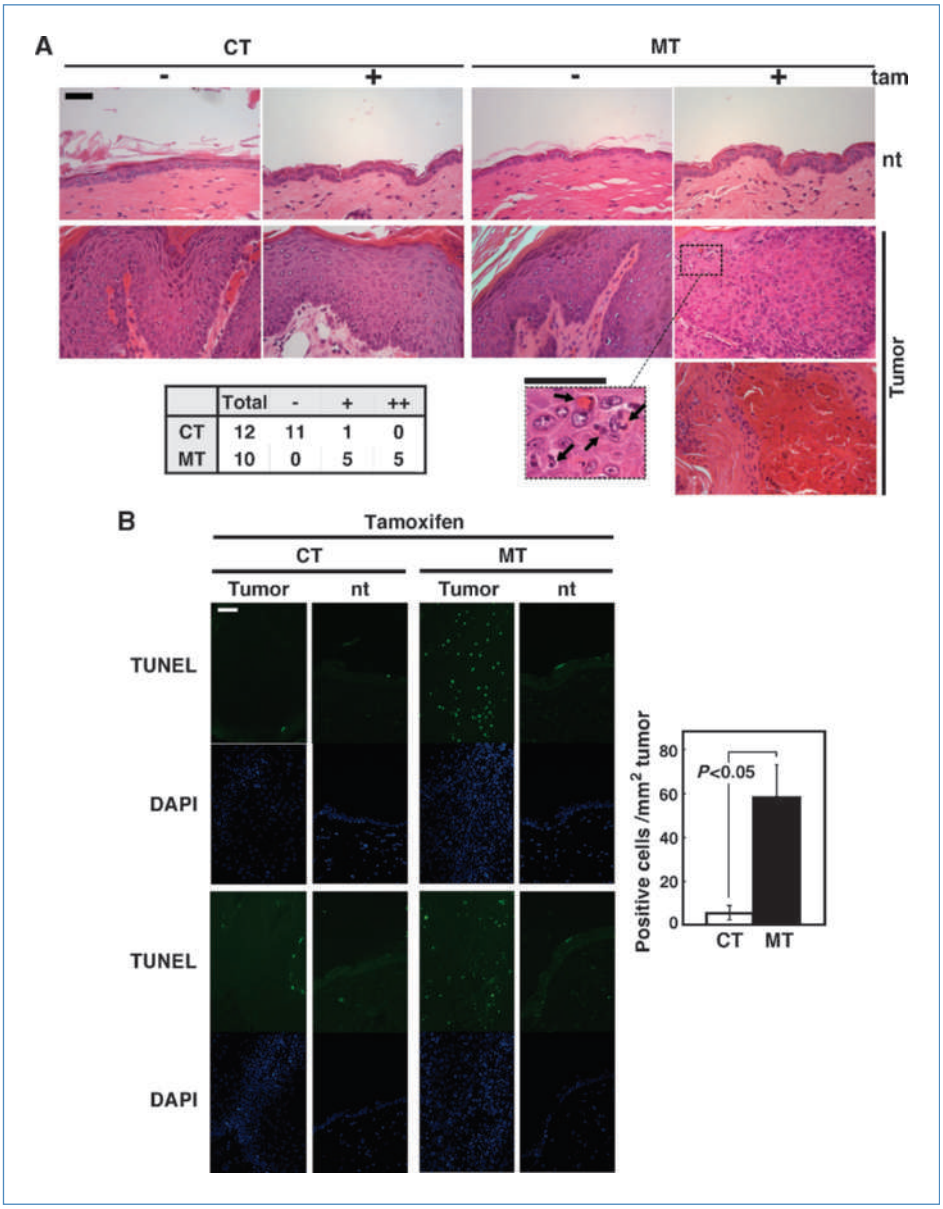

Figure 2. Ablation of TAK1 upregulates apoptosis in tumors. Tumors and normal skin [normal tissue (nt)] regions of the skin of *TAK1*$^{flox/flox}$ (CT) and *K14-CreERT TAK1* $^{flox/flox}$ (MT) mice were harvested when tumors started regressing at days 3 to 6 after the tamoxifen treatment. H&E (A) and TUNEL (B) staining was performed with Bouin-fixed sections. A, bottom, tumors that lost cellularity. Arrows indicate fragmented nuclei. Tumors are categorized according to the level of apoptotic cells (bottom left table): –, no apoptotic cells; +, ≥10% tumor cells are apoptotic; ++, loss of cellularity similar to the bottom panel image. Scale bar, 40 μm. B, DAPI staining (blue) images (second and fourth panels) are shown in the same fields of TUNEL staining (green) images (first and third panels). Data are representative images of tumors and normal regions of two different mice. TUNEL-positive cells in tumors were counted using CT and MT. Columns, mean (n = 3); bars, SE. Scale bar, 40 μm.

paraffin sections using an apoptotic cell death detection kit (Promega) according to the manufacturer's instructions. Sections were counterstained with 4′,6-diamidino-2-phenylindole (DAPI).

Quantitative real-time PCR

Total RNA from keratinocytes was isolated using RNeasy Mini (Qiagen). cDNA was synthesized using Taqman reverse transcription reagents (Applied Biosystems). mRNA levels of NAD(P)H:quinone oxidoreductase 1 (NQO1) and glyceraldehyde-3-phosphate dehydrogenase (GAPDH) were analyzed by real-time PCR with SYBR Green (Applied Biosystems). NQO1 primers (CATTCTGAAAGGCTGGTTTGA and CTAGCTTTGATCTGGTTGTCAG) and GAPDH primers (GAAGGTCGCTGTGAACGGA and GTTAGTGGGGTCTCGCTCCT) were used. Expression levels of GSTP1, GSTM1, glutamylcysteine ligase catalytic subunit (GCLC), MIP2, and GAPDH were also analyzed by Taqman gene expression assay (Applied Biosystems). Results were analyzed using the comparative C_t method. Values were normalized to the level of GAPDH mRNA.

ROS measurement

For ROS measurement in skin tumors and normal skin, harvested skin was embedded and frozen in OCT compound and sections were prepared. Sections were stained with 5 μmol/L CM-H2DCFDA (Invitrogen) for 1.5 hours at 37°C. Images were taken using a fluorescent microscope (BX41, Olympus) controlled by IPlab (Scanalytics). Randomly selected areas were photographed with the same exposure time. The images were processed using the same fixed

Table 1. Papillomas before and after *tak1* gene deletion

Genotype	1–3 mm		>3 mm	
	Before	After	Before	After
Experiment 1*				
TAK1$^{flox/flox}$	10	5	8	9†
K14-CreERT TAK1$^{flox/flox}$	35	0	15	0
Experiment 2‡				
TAK1$^{flox/flox}$	69	57	15	10
K14-CreERT TAK1$^{flox/flox}$	39	5	28	2

*Single-time DMBA-treated mice were treated with TPA for 27 wk and subsequently injected 1 mg/mouse tamoxifen for 5 consecutive days. The total number of papillomas in three *TAK1*$^{flox/flox}$ and seven *K14-CreERT TAK1*$^{flox/flox}$ mice was counted before tamoxifen injection and 14 d after the completion of tamoxifen injection.
†One tumor was getting bigger after tamoxifen treatment.
‡Single-time DMBA-treated mice were treated with TPA for 22 wk and subsequently injected with 1 mg/mouse tamoxifen for 5 consecutive days. The total number of papillomas in six *TAK1*$^{flox/flox}$ and six *K14-CreERT TAK1*$^{flox/flox}$ was counted before tamoxifen injection and 4 d after the completion of tamoxifen injection.

threshold in all samples by Photoshop software, and representative images are shown.

Transient small interfering RNA system

Nontargeting control small interfering RNAs (siRNA) were purchased from Dharmacon (Nontargeting siRNA#1), and siRNAs targeted against TAK1 were generated (siTAK1#2, 5′-GAGAUCGACUACAAGGAGA-3′; siTAK1#3, 5′-GGCAAAGCAACAGAGUGAAUCUGGA-3′). T24 cells were transfected with siRNAs by using Lipofectamine 2000 reagent (Invitrogen).

Immunoblotting

T24 cells were washed once with ice-cold PBS, and whole-cell extracts were prepared using a lysis buffer [20 mmol/L HEPES (pH 7.4), 150 mmol/L NaCl, 12.5 mmol/L β-glycerophosphate, 1.5 mmol/L $MgCl_2$, 2 mmol/L EGTA, 10 mmol/L NaF, 2 mmol/L DTT, 1 mmol/L Na_3VO_4, 1 mmol/L phenylmethylsulfonyl fluoride, 20 μmol/L aprotinin, 0.5% Triton X-100]. Cell extracts were resolved on SDS-PAGE and transferred to Hybond-P membranes (GE Healthcare). The membranes were immunoblotted with various antibodies, and the bound antibodies were visualized with horseradish peroxidase–conjugated antibodies against rabbit or mouse IgG using the ECL or ECL advance Western blotting detection kit (GE Healthcare).

Annexin V–binding assay

To determine apoptosis, Annexin V–Alexa Fluor 488 binding was performed according to the manufacturer's protocol (Invitrogen). Fluorescence was detected by flow cytometry and analyzed by FlowJo software (Tree Star, Inc.).

Statistical analyses

Statistical comparisons were made using Student's *t* test or log-rank test.

Results and Discussion

Ablation of TAK1 causes regression of skin tumors *in vivo*

Mice having constitutive epidermal-specific deletion of TAK1 (*K5-Cre TAK1*$^{flox/flox}$) develop severe skin damage at neonatal days 5 to 7 and are lethal around postnatal days 7 to 8 (10). We have found that this damage is blocked by deletion of TNF receptor 1 gene (TNFR1$^{-/-}$). TNF is constantly expressed at some levels in the normal skin, and when TAK1 is ablated, TNF upregulates ROS, resulting in apoptosis (9, 10). By using an inducible epidermal-specific gene deletion system (*K14-CreERT TAK1*$^{flox/flox}$), we have examined the role of TAK1-ROS pathway in adult mouse skin. In adult mice, TAK1 deficiency modestly increases apoptosis; however, it does not cause severe skin damage as observed in the neonatal TAK1 mutant mice. Therefore, TAK1 is important but not critically involved in cell survival in the normal adult epidermis. We then asked whether epidermal-derived tumor cells *in vivo* are more sensitive to TAK1 ablation. We used inducible epidermal-specific TAK1 knockout (*K14-CreERT TAK1*$^{flox/flox}$) mice and examined the effect of TAK1 deletion in preexisting epidermal-derived tumors. Skin tumors were induced by initiation with DMBA and promotion with TPA (18). *tak1* gene deletion was induced by 5-consecutive-day treatment of 0.5 to 1 mg/mouse/day tamoxifen. This treatment regimen induced *tak1* gene deletion in both tumors and normal regions of the skin (Fig. 1A) and did not cause extensive apoptosis in the normal epidermis (Fig. 2B). We performed four independent experiments, and all skin tumors on *K14-CreERT TAK1*$^{flox/flox}$ mice disappeared within 5 to 13 days after tamoxifen treatment (n = 20; Fig. 1B and C; Table 1). In comparison, few tumors regressed in tamoxifen-treated control *TAK1*$^{flox/flox}$ mice (n = 14; Fig. 1B and C; Table 1). TAK1-deleted tumors started regressing at 3 days after the completion of tamoxifen treatment (day 3). Histologic analysis revealed that TAK1-deficient tumors contained large numbers of cells having fragmented nuclei (Fig. 2A) and exhibited extensive apoptosis (Fig. 2B) at days 3 to 6. In comparison, no pronounced increased apoptosis or tissue damages were observed in normal skin (Fig. 2A and B). TAK1-deficient tumors lost cellularity starting from day 6 (Fig. 2A, bottom). These results show that ablation of TAK1 is selectively cytotoxic to epidermal-derived tumors.

Cell proliferation is not affected by ablation of TAK1

To determine the mechanism by which ablation of TAK1 causes tumor regression, we examined whether ablation of TAK1 impairs tumor cell proliferation. BrdUrd incorporation was examined in control and TAK1-deficient epidermis in mice with skin tumors. Cell proliferation was not altered

by TAK1 deletion in tumors or normal epidermis (Fig. 3). This indicates that the TAK1 pathway is not important for tumor cell proliferation, and that the cause of tumor regression is not due to impaired cell proliferation.

ROS is upregulated in TAK1-deficient skin tumors

We have previously shown that TAK1–c-Jun pathway regulates the levels of ROS in keratinocytes (9). To further investigate the mechanism by which TAK1 regulates antioxidant capacity in keratinocytes, we examined the expression levels of several cellular antioxidant genes with and without TNF stimulation (Fig. 4A). Among the antioxidant genes we examined, the mRNA levels of NQO1, glutathione *S*-transferases (GSTM1 and GSTP1), and GCLC were reduced by TAK1 ablation in both unstimulated and TNF-stimulated keratinocytes. However, other antioxidant genes such as manganese superoxide dismutase (MnSOD) were found to be unchanged by TAK1 ablation (9). Thus, ablation of TAK1 downregulates the levels of a subset of cellular antioxidant genes and lowers cellular antioxidant capacity in keratinocytes. We attempted to analyze the levels of the above cellular antioxidant genes in tumors; however, we were unable to obtain enough RNA from TAK1-deficient tumors because the tumors were highly apoptotic. We anticipate that the ablation of TAK1 reduces antioxidant capacity in tumors as observed in normal keratinocytes, and that the ROS levels might be higher in tumors due to increased production of ROS in tumor cells. We tested the levels of ROS in skin tumors by staining with the ROS-reactive

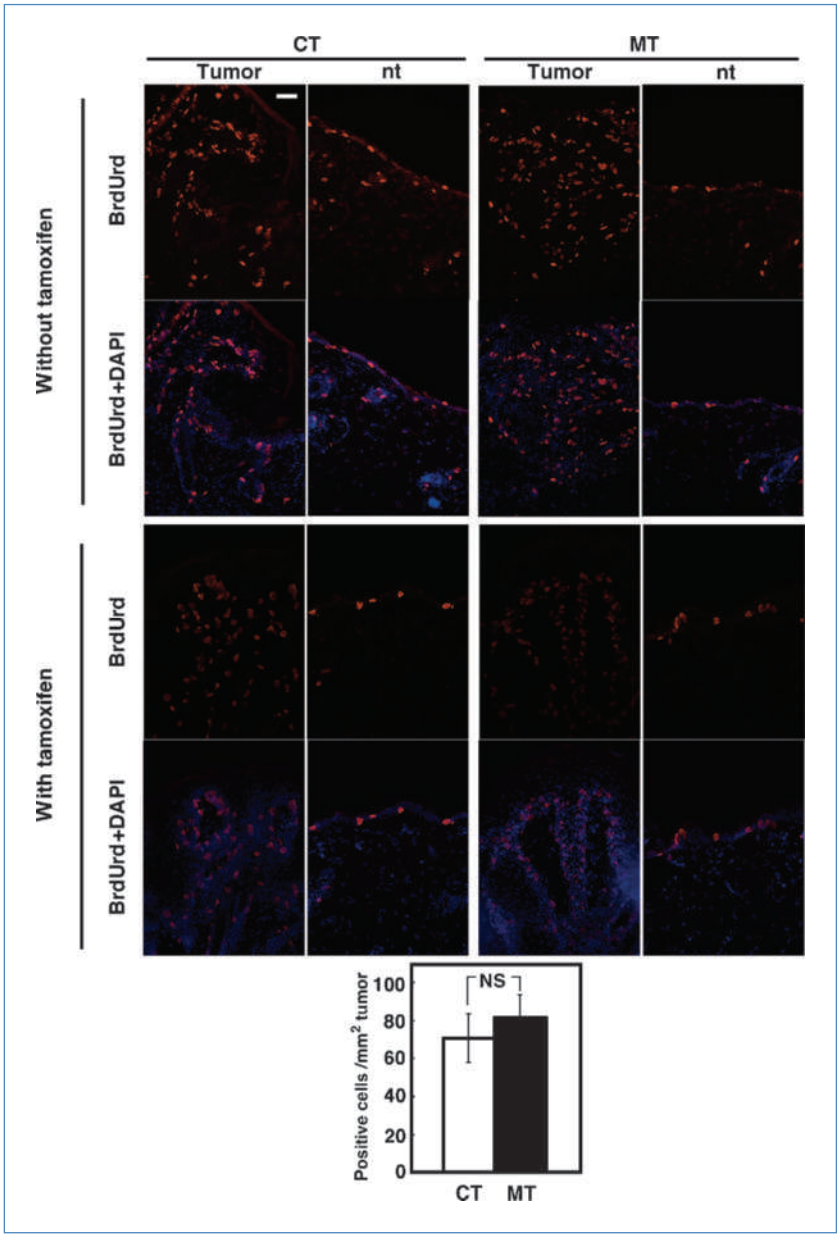

Figure 3. Ablation of TAK1 does not affect cell proliferation. *TAK1*$^{flox/flox}$ (CT) and *K14-CreERT TAK1* $^{flox/flox}$ (MT) mice having skin papillomas were treated with tamoxifen (0.5 mg/mouse/day) for 5 consecutive days. Mice with or without tamoxifen treatment at day 6 were injected with 0.1 mg/g of BrdUrd 1.5 h before samples were harvested, and frozen sections were subjected to immunohistochemical analysis using anti-BrdUrd antibody in tumors or normal region of the skin (nt). Scale bar, 40 μm. The analysis was done in two independent experiments, and photomicrographs of representative images of tumors and normal regions are shown. BrdUrd-positive cells in tumors were counted. Columns, mean (CT, $n = 5$; MT, $n = 6$); bars, SE; NS, not significant.

dye CM-H2DCFDA at days 3 to 6 (Fig. 4B). TAK1-deficient tumors accumulated high levels of ROS, whereas normal skin with *tak1* gene deletion or tumors in control mice exhibited only marginal or no accumulation of ROS compared with the control normal skin in $TAK1^{flox/flox}$ mice (Fig. 4B). Tumors harvested before *tak1* gene deletion did not exhibit ROS accumulation (Fig. 4C), indicating that increased ROS was caused by *tak1* gene deletion. These results are consistent with the idea that the ablation of TAK1 in tumor cells reduces their antioxidant capacity resulting in increased ROS, which causes tumor cell apoptosis.

Ablation of TAK1 causes hypersensitivity to apoptosis in T24 cells

Our results thus far show that skin tumor regression is correlated with TAK1 deficiency-dependent apoptosis. To

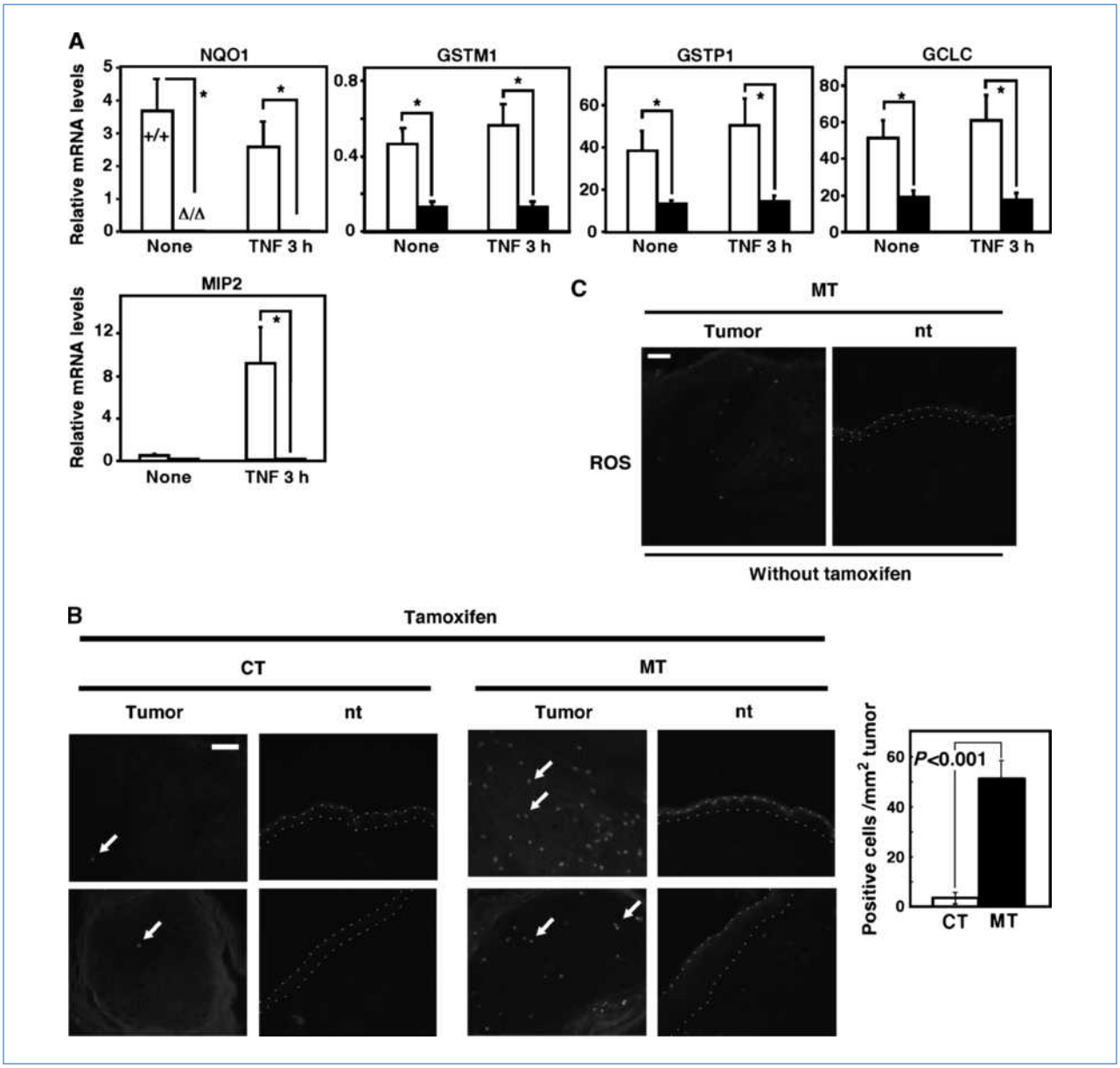

Figure 4. Ablation of TAK1 upregulates ROS in tumors. A, real-time PCR analysis to quantify mRNA levels in TAK1 wild-type (+/+) and Δ/Δ keratinocytes. Keratinocytes were left untreated or treated with 20 ng/mL TNF for 3 h. MIP2 was used as a control for TNF-responsive genes. Relative mRNA levels were calculated using GAPDH mRNA. Columns, mean (NQO1, $n = 4$; GSTM1, $n = 4$; MIP2, GSTP1, and GCLC, $n = 10$); bars, SE. *, $P < 0.05$. B, ROS were detected in unfixed fresh-frozen sections from $TAK1^{flox/flox}$ (CT) and *K14-CreERT* $TAK1^{flox/flox}$ (MT) mice by CM-H2DCFDA. Arrows indicate examples of CM-H2DCFDA–positive cells. Photomicrographs are representative images of tumors and normal regions of two different mice. Scale bars, 40 μm. ROS-positive cells in tumors were counted. Columns, mean (CT, $n = 5$; MT, $n = 9$); bars, SE. C, sections from tumors and normal regions of the skin of *K14-CreERT* $TAK1^{flox/flox}$ (MT) mice without tamoxifen treatment. ROS staining of unfixed frozen sections using CM-H2DCFDA is shown. Scale bar, 40 μm.

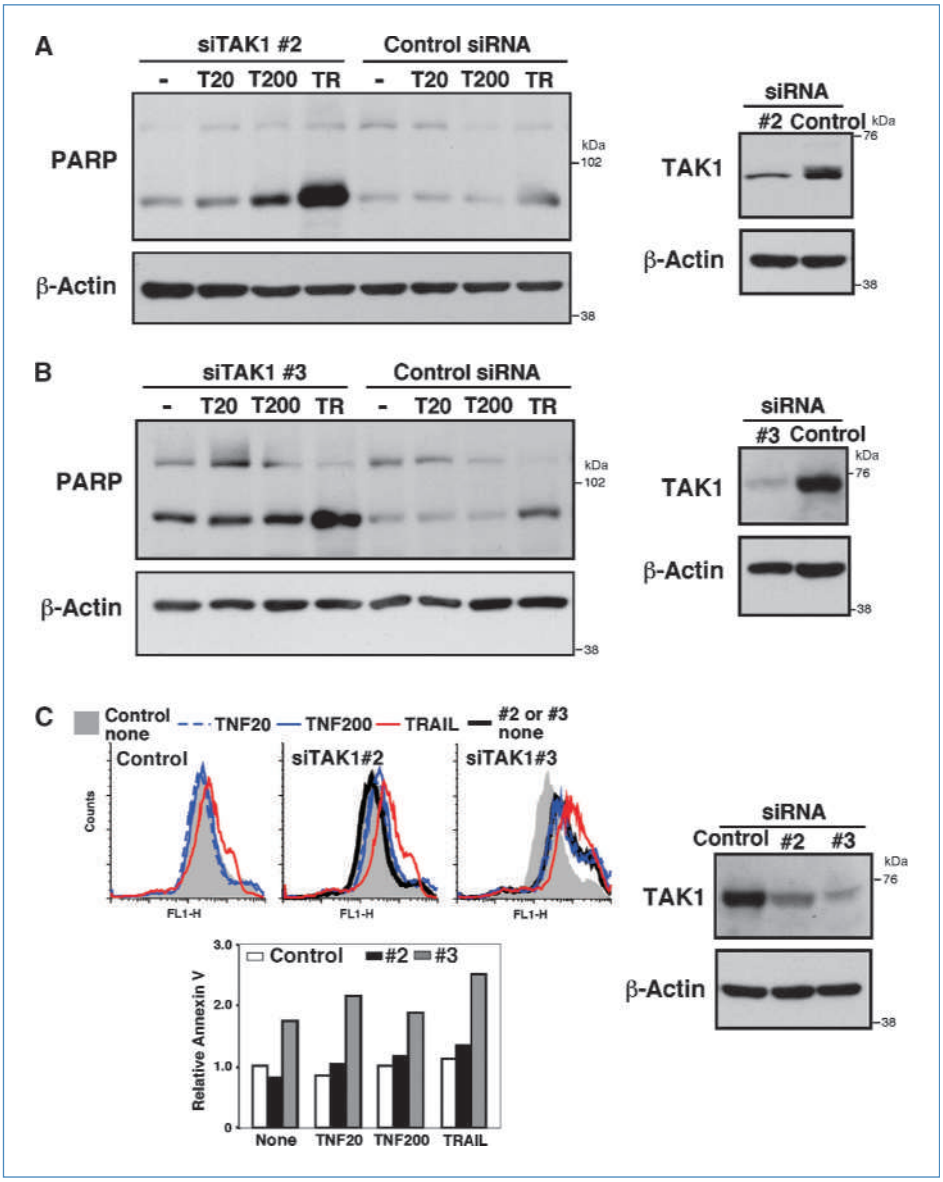

Figure 5. Ablation of TAK1 in H-Ras–transformed cells causes cell death. A and B, T24 cells were transfected with nontarget siRNA (control) or TAK1-targeted siRNAs [siTAK1#2 (A) and siTAK1#3 (B)] and stimulated with 20 ng/mL TNF (T20) and 200 ng/mL TNF (T200) for 4.5 h (A) or 10 h (B) or with 100 ng/mL TRAIL (TR) for 4.5 h (A) or 2 h (B). Cell lysates were analyzed by immunoblotting with anti-TAK1 and anti-PARP. C, T24 cells were transfected with nontarget, siTAK#2 or siTAK1#3, and stimulated with 20 ng/mL TNF and 200 ng/mL TNF for 10 h or with 100 ng/mL TRAIL for 2 h. Apoptotic cells were analyzed by Annexin V–binding assay. Left, top, staining of unstimulated nontarget siRNA cells in gray shadow in all three panels; bottom, fluorescence units relative to that of unstimulated nontarget siRNA. Right, TAK1 expression was analyzed by immunoblotting with anti-TAK1. Data are representative of two independent experiments with similar results.

further verify whether ablation of TAK1 can directly kill tumor cells, we used cultured cells. DMBA-TPA skin tumors are highly associated with oncogenic mutations in Ras, specifically in H-Ras (18–20). We therefore examined whether TAK1 deficiency can cause apoptosis in a tumor cell line having the H-Ras oncogenic mutation. We used T24 tumor cell line, which possesses the oncogenic H-Ras G12V mutation, and tested the effect of TAK1 knockdown. Nontarget siRNA and two different siRNAs against human TAK1 (siTAK1#2 and siTAK1#3) were transfected into T24 cells, and cells were treated with apoptosis inducers TNF and TRAIL (TNF-related apoptosis-inducing ligand). Caspase activation was analyzed by cleavage of PARP, and Annexin V binding was also analyzed. In control siRNA–treated T24 cells, TRAIL slightly increased cleaved PARP and Annexin V binding, whereas TNF had no effect (Fig. 5A–C). TAK1 siRNA (siTAK1#2) reduced the levels of TAK1 (Fig. 5A, right) and increased cleaved PARP on TNF and TRAIL treatment (Fig. 5A). siTAK1#2 also slightly increased Annexin V binding (Fig. 5C). The other TAK1 siRNA (siTAK1#3) effectively reduced the level of TAK1 and highly increased cleaved PARP and Annexin V binding (Fig. 5B and C). We note that we observed morphologic changes consistent with apoptotic cells (shrinking cells) in T24 cells expressing siTAK1#3 even in the absence of TNF or TRAIL, and we could detect cleaved PARP in unstimulated cells (Fig. 5B, most left lane). These results indicate that the level of TAK1 is correlated with resistance to apoptosis in tumor cells having H-Ras mutation.

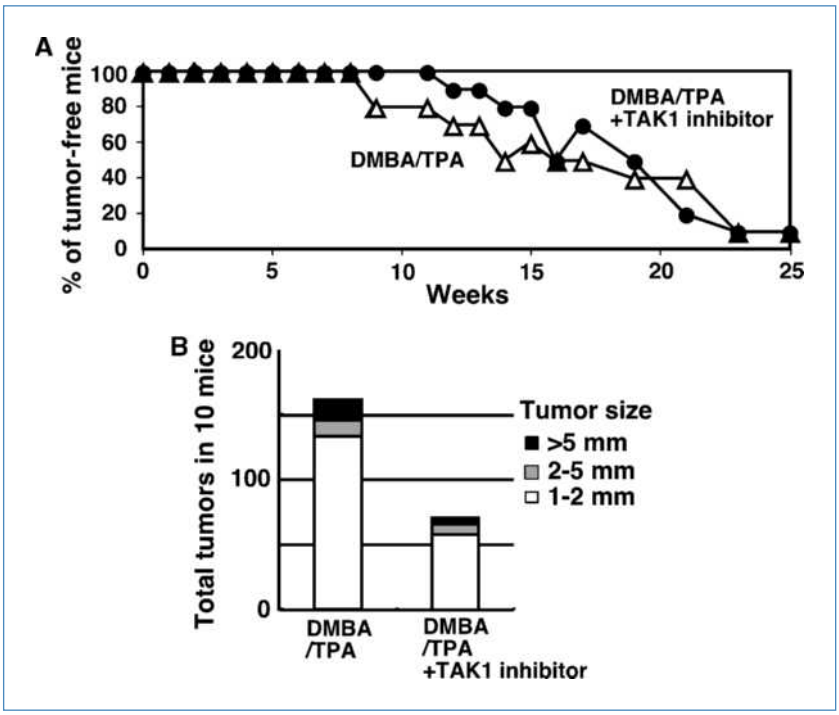

Figure 6. TAK1 inhibitor inhibits skin tumorigenesis. CD1 mice (n = 10 for each treatment) were treated with a single application of 200 nmol DMBA followed 1 wk later with twice weekly treatment of 5 nmol TPA for 25 wk. Control vehicle (acetone) or 100 nmol 5Z-7-oxozeaenol was administered topically 30 min before every TPA treatment. A, the number of mice having tumors (>1 mm) was counted every week. P = 0.88 (not significant difference) by log-rank test. B, the total numbers of tumors at 25 wk of TPA treatment were analyzed. 5Z-7-oxozeaenol treatment alone without DMBA or TPA did not induce skin papilloma or any skin abnormality.

A selective TAK1 inhibitor downregulates skin tumor development

We also wanted to examine whether ablation of TAK1 could block tumor development. However, we found that induction of *tak1* gene deletion together with the tumor promoter TPA treatment caused a severe inflammatory condition in normal epidermis, which precluded the use of these mice. We speculated that complete deletion of TAK1 strongly enhances TPA-induced inflammation. We therefore chose to use a selective TAK1 inhibitor, 5Z-7-oxozeaenol (17), which partially blocks TAK1 activity. We examined whether inhibition of TAK1 activity could reduce tumor development in DMBA-TPA mouse skin tumor models (Fig. 6). After the initiation of tumors by DMBA treatment, 5Z-7-oxozeaenol or vehicle was applied to the skin 30 minutes before each TPA treatment. The tumor incidence was not significantly altered by 5Z-7-oxozeaenol treatment (Fig. 6A). However, 10 mice with vehicle treatment developed total 160 tumors at 25 weeks, whereas only 71 was observed in 10 mice with 5Z-7-oxozeaenol treatment (Fig. 6B). These results suggest that inhibition of TAK1 kinase may inhibit tumor development at least in the mouse skin tumor model. Although these results raise the possibility that the TAK1 inhibitor may be useful to treat tumors, 5Z-7-oxozeaenol is a selective but not specific inhibitor of TAK1, which may cause side effects. We note here that treatment of preexisting tumors with 5Z-7-oxozeaenol did not alter the size of tumors, suggesting that a stronger inhibition of TAK1 may be required for regression of preexisting tumors.

Highly proliferating cells such as tumor cells produce more ROS compared with normal tissues due to increased activity in the respiratory chain, and balance the ROS levels by upregulating cellular antioxidant capacity. TAK1 ablation-mediated reduction of cellular antioxidant capacity highly affects tumors, which results in the selective killing of tumor cells. TAK1 is an essential intermediate activating transcription factor of NF-κB and AP1, and both are involved in the transcriptional regulation of several genes associated with cell survival (21–23). NF-κB and AP1 regulate antiapoptotic genes and cellular antioxidant genes. Therefore, it is likely that TAK1 regulation of both NF-κB and AP1 plays a central role in tumor cell survival not only by reducing ROS but also by inducing antiapoptotic genes. Approaches to inhibit TAK1 signaling might provide a new avenue of cancer therapy.

Disclosure of Potential Conflicts of Interest

No potential conflicts of interest were disclosed.

Acknowledgments

We thank S. Akira for TAK1-floxed mice and B.J. Welker and M. Mattmuler for support.

Grant Support

NIH grants GM068812 and GM084406 (J. Ninomiya-Tsuji).

The costs of publication of this article were defrayed in part by the payment of page charges. This article must therefore be hereby marked *advertisement* in accordance with 18 U.S.C. Section 1734 solely to indicate this fact.

Received 04/08/2010; revised 08/02/2010; accepted 08/05/2010; published OnlineFirst 10/19/2010.

References

1. Shim JH, Xiao C, Paschal AE, et al. TAK1, but not TAB1 or TAB2, plays an essential role in multiple signaling pathways *in vivo*. Genes Dev 2005;19:2668–81.
2. Takaesu G, Ninomiya-Tsuji J, Kishida S, Li X, Stark GR, Matsumoto K. Interleukin-1 (IL-1) receptor-associated kinase leads to activation of TAK1 by inducing TAB2 translocation in the IL-1 signaling pathway. Mol Cell Biol 2001;21:2475–84.
3. Ninomiya-Tsuji J, Kishimoto K, Hiyama A, Inoue J, Cao Z, Matsumoto K. The kinase TAK1 can activate the NIK-IκB as well as the MAP kinase cascade in the IL-1 signalling pathway. Nature 1999;398:252–6.
4. Liu HH, Xie M, Schneider MD, Chen ZJ. Essential role of TAK1 in thymocyte development and activation. Proc Natl Acad Sci U S A 2006;103:11677–82.
5. Wan YY, Chi H, Xie M, Schneider MD, Flavell RA. The kinase TAK1 integrates antigen and cytokine receptor signaling for T cell development, survival and function. Nat Immunol 2006;7:851–8.
6. Sato S, Sanjo H, Takeda K, et al. Essential function for the kinase TAK1 in innate and adaptive immune responses. Nat Immunol 2005;6:1087–95.
7. Pasparakis M. Regulation of tissue homeostasis by NF-κB signalling: implications for inflammatory diseases. Nat Rev Immunol 2009;9:778–88.
8. Kajino-Sakamoto R, Inagaki M, Lippert E, et al. Enterocyte-derived TAK1 signaling prevents epithelium apoptosis and the development of ileitis and colitis. J Immunol 2008;181:1143–52.
9. Omori E, Morioka S, Matsumoto K, Ninomiya-Tsuji J. TAK1 regulates reactive oxygen species and cell death in keratinocytes, which is essential for skin integrity. J Biol Chem 2008;283:26161–8.
10. Omori E, Matsumoto K, Sanjo H, et al. TAK1 is a master regulator of epidermal homeostasis involving skin inflammation and apoptosis. J Biol Chem 2006;281:19610–7.
11. Trachootham D, Alexandre J, Huang P. Targeting cancer cells by ROS-mediated mechanisms: a radical therapeutic approach? Nat Rev Drug Discov 2009;8:579–91.
12. Dolado I, Nebreda AR. AKT and oxidative stress team up to kill cancer cells. Cancer Cell 2008;14:427–9.
13. Nogueira V, Park Y, Chen C-C, et al. Akt determines replicative senescence and oxidative or oncogenic premature Senescence and sensitizes cells to oxidative apoptosis. Cancer Cell 2008;14:458–70.
14. Trachootham D, Zhou Y, Zhang H, et al. Selective killing of oncogenically transformed cells through a ROS-mediated mechanism by β-phenylethyl isothiocyanate. Cancer Cell 2006;10:241–52.
15. Diehn M, Cho RW, Lobo NA, et al. Association of reactive oxygen species levels and radioresistance in cancer stem cells. Nature 2009;458:780–3.
16. Vasioukhin V, Degenstein L, Wise B, Fuchs E. The magical touch: genome targeting in epidermal stem cells induced by tamoxifen application to mouse skin. Proc Natl Acad Sci U S A 1999;96:8551–6.
17. Ninomiya-Tsuji J, Kajino T, Ono K, et al. A resorcylic acid lactone, 5Z-7-oxo-zeaenol, prevents inflammation by inhibiting the catalytic activity of TAK1 MAPKKK. J Biol Chem 2003;278:18485–90.
18. Balmain A, Pragnell IB. Mouse skin carcinomas induced *in vivo* by chemical carcinogens have a transforming Harvey-ras oncogene. Nature 1983;303:72–4.
19. Loomis KD, Zhu S, Yoon K, Johnson PF, Smart RC. Genetic ablation of CCAAT/enhancer binding protein α in epidermis reveals its role in suppression of epithelial tumorigenesis. Cancer Res 2007;67:6768–76.
20. Brown K, Buchmann A, Balmain A. Carcinogen-induced mutations in the mouse c-Ha-ras gene provide evidence of multiple pathways for tumor progression. Proc Natl Acad Sci U S A 1990;87:538–42.
21. Karin M, Lin A. NF-κB at the crossroads of life and death. Nat Immunol 2002;3:221–7.
22. Micheau O, Lens S, Gaide O, Alevizopoulos K, Tschopp J. NF-κB signals induce the expression of c-FLIP. Mol Cell Biol 2001;21:5299–305.
23. Gerald D, Berra E, Frapart YM, et al. JunD reduces tumor angiogenesis by protecting cells from oxidative stress. Cell 2004;118:781–94.